Atlantis Highlights in Engineering, volume 6
14th International Renewable Energy Storage Conference 2020 (IRES 2020)

Hybrid Electrical Storage Solutions for Developing Reliable Transport Systems

Paul Nicolae BORZA
Electronics and Computers
Transilvania University of Brasov
Brasov, Romania
borzapn@unitbv.ro

Mihai MACHEDON-PISU
Electronics and Computers
Transilvania University of Brasov
Brasov, Romania
mihai_machedon@unitbv.ro

Marius Catalin CARP
Electronics and Computers
Transilvania University of Brasov
Brasov, Romania
marius.carp@unitbv.ro

***Abstract*—Hybrid Electrical Storage could be considered a solution for developing sustainable transportation systems. But, are they reliable? In terms of life span, reliability, availability, and range, conventional vehicles such as cars, buses, trains are better than electrical or hybrid ones. However, traditional transportation systems present increased energy consumption and low energy efficiency. Also, the impact on environment and health could be more negative than the electrical and hybrid ones. In this paper we test if it is possible to reach a compromise between sustainability and technology constraints by developing a reliable hybrid transportation system with improved life span and range. In this sense, two designs have been implemented: a hybrid starting system for a locomotive and a hybrid storage solution for an e-bike. Both are made of batteries, supercapacitors, and the corresponding power electronics, allowing the optimal control of power flows between the system's components and actuators. The proposed designs meet the application's requirements in terms of functional and sustainability goals. Our analysis is based on power electronics, complexity, energy efficiency and temperature range considerations. The hybrid storage system used for starting the locomotive's Diesel engine was tested under various real operating conditions and has shown no failure, emphasizing its performance in terms of availability, reliability and life span. The prototype for the hybrid e-bike does not depend on battery operation for short periods of time and costs less than a normal e-bike. Also, in comparison to the latter, it has better autonomy and better energy efficiency.**

Keywords—hybrid energy storage systems, sustainable transportation, batteries, supercapacitors

I. MOTIVATION

In order to provide an appropriate design of sustainable transportation systems, that could reduce the dependency on oil (gasoline and diesel), storage solutions such as batteries, supercapacitors (SC), and fuel cells (FC) [1, 2] must be adapted accordingly in order to deliver at least acceptable autonomy and lifetime while reducing maintenance and operation costs and impact on environment [3, 4, 5]. The power and energy densities of the main types of electric storage, according to the characteristics detailed in Ragone plots [3], emphasize on the range (cycle life) associated to specific energy, and acceleration, associated to specific power [6, 7, 8]. While internal combustion engine vehicles (ICEVs) provide the necessary range and acceleration that can satisfy the demands of the trip (e.g., 500 km range), neither of the vehicles based on electric storage solutions (ESS) can respond to such demands [2, 3, 5, 6]. Also, the lifetime of vehicles based on ESS is limited and must also deal with the impact of temperature, voltage and current on the operation cycle. In this sense, hybridization of the electric sources can be seen as a solution, as proven in [9]. Although vehicles based on hybrid electric storage systems (HESS) are shown to have better energy efficiency than ICEVs and reduce the fuel consumption, questions regarding reliability and availability still remain [10]. We try to show that, by appropriate sizing and hybridization of the electrical storage components, acceptable range and lifetime can be reached, while the reliability of the proposed vehicle is improved by assuring a coherent power flow between the two electric storage elements: batteries and SC.

II. STORAGE SOLUTIONS & APPLICATION DEMANDS

A. Storage solutions for HESS

EESs are mostly based on electrochemical technologies. These are mainly Lead-acid, Lithium-ion, and Nickel-cadmium (Ni-Cd) and Nickel-metal hybride (Ni-MH) batteries. Their main characteristics are presented in Table 1. Other commercialized batteries are based on Sodium, such as sodium sulfur (NaS) and sodium nickel chloride (e.g., ZEBRA), while other types are yet to be developed at large scale, such as flow batteries based on: vanadium redox (VRB), zinc bromine (ZnBr), and polysulfide bromine (PSB) [1].

TABLE I. MAIN BATTERY TYPES

Metric	**Batteries based on Lithium, Nickel and Lead**		
	Lithium-Ion	***Ni-MH & Ni-Cd***	***Lead Acid***
Specific energy (Wh/kg)	75–200[a]; 150–350[a]	70–100[a]; 20–240[b]	20–40[a]; 25–50[a]
Specific power (W/kg)	300–800[a]	130–500[a]	75–300[a]
Cell voltage (V)	3.6[a]	1.2[a]	2.1[a]
Life cycles (cycles)	500[a];1500–4500[a];1000[b]	2000[a];600–2000[b]	200–1800[a];1000[b]
Temperature of operation (°C)	-20–55[a]	-20–50[a]	-30–60[a]
Discharge time at power rating (sec. to h.)	minutes-h., 1–8 h[a]	sec.-h., 1–8 h[a]	sec.-h., up to 10 h[a]
Self-discharge (%/Day)	0.1–5[a]	0.03–0.6[a]	0.1–0.3[a]

Metric	Batteries based on Lithium, Nickel and Lead		
	Lithium-Ion	*Ni-MH & Ni-Cd*	*Lead Acid*
Overall efficiency (%)	85–95[a]	60–73[a]; 80[a]	70–90[a]
Capital cost (€/kW)	800-3600[a]	450-1350[a]	180-550[a]
Capital cost (€/kWh)	550-3500[a]	350-2150[a]	45-350[a]

[a.] According to [1, 2, 3, 4].

[b.] According to [6, 11].

On the other hand, there are also other EES technologies, such as the mechanical (e.g., flywheel), thermo mechanical (solar fuels), chemical (e.g., hydrogen fuel cells FC), electrical (e.g., supercapacitor SC) and thermal (heat storage) ones [1]. By integrating two different EES technologies into one application it can be proven beneficial to develop a HESS. Such HESS combinations are based on the batteries discussed in Table 1 and double layer capacitors, known also as SC. The main SC types are analyzed in Table 2.

TABLE II. MAIN SC TYPES

Metric	EDLC, pseudo & hybrid SC types		
	EDLC	*Pseudo*	*Hybrid asymmetric*
Specific energy (Wh/kg)	3–5[a]; 5–20[a]	10[a]	180[a]; 20–30[b]
Specific power (W/kg)	500–10,000[a]; 800–23,500[a]		
Cell voltage (V)	2.5[a]; 2.7[a]	2.3–2.8[a]	2.3–2.8[a]
Life cycles (cycles)	1,000,000[a]	100,000[a]	500,000[a]
Temperature of operation (°C)	-30–65[a]; -40–65[a]	-40–65[a]	-40–65[a]
Discharge time at power rating (msec. to h.)	msec.–1h[a].;1sec.-100sec.[a]		
Self-discharge (%/Day)	5-40[a]		-

[a.] According to [1, 3, 4].

[b.] According to [7].

Another possibility refers to hydrogen EES in order to provide electricity. In Table 3 hydrogen FCs are compared to the main battery and SC types.

TABLE III. MAIN TYPES OF ELECTRIC ENERGY STORAGE

Metric	Main types		
	Main types of Battery	*Main SCs*	*Hydrogen FC*
Specific energy (Wh/kg)	20–350[a]	3–30[b]	150–1500[a]
Specific power (W/kg)	75–800[a]	500–23500[a]	5–800[a]
Cell voltage (V)	1.2–3.6[a]	2.3–2.8[a]; 2.5–3.7[b]	-
Life cycles (cycles)	500–2000[b]	100,000–1,000,000[a]	1000–20,000+[a]
Temperature of operation (°C)	-20–60[a]	-40–65[a]	-
Discharge time at power rating (msec. to h.)	sec.-hours, 1–10h[a]	msec. –100 sec.[a,b]	sec.-24h+[a]
Self-discharge (%/Day)	0.03–5[a]	5-40[b]	Negligible[a]

Metric	Main types		
	Main types of Battery	*Main SCs*	*Hydrogen FC*
Overall efficiency (%)	60–90[a]	95–97[a]	20–66[a]
Capital cost (€/kW)	180-3600[a]	90–400[a] (EDLC)	500–4700[a]; 500-3000[a]
Capital cost (€/kWh)	45-3500[a]	250–1800[a] (EDLC)	400–780[a]

[a.] According to [1, 2, 3, 4].

[b.] According to [6, 7, 11].

There are also other characteristics which can prove just as relevant to the HESS application: power and energy capacity ratings (in MW and MWh), lifetime (in years), operating and maintenance costs, and maturity [1].

B. Impact of application demands on HESS

One way to analyze the application requirements is based on duration and usage frequency: from short duration (10 years) with highly frequent usage (discharge time: minutes to half an hour) to medium and long duration (15-20 years) with fast response and frequent usage (discharge time: hours) [4]. While Lead-acid can be seen as an ideal candidate in most cases, Li-ion is better for short and medium term and Ni-Cd for long term. There is also another case, when the usage is much more frequent (discharge time: milliseconds to seconds) [12], like in the case of a starting system of a vehicle. For such fast charge and discharge times, only SCs can meet such application demands, as seen in Tables 2-3. In terms of temperature performance, cycle efficiency [13], and costs of power and energy, storage components such as Lead-acid, Li-ion, and SCs [14, 15] can be seen as primary candidates for vehicle propulsion [11].

The HESS can be used in applications that deal in general with significant and frequent variations of load demands of the vehicle acting system. Also, some applications that require frequent conversions of mechanical, radiant or chemical energy into electrical energy or vice versa can be implemented by using HESS. In this case, HESS is composed of batteries, which are medium release storage devices, and supercapacitors, which are fast release storage devices. Batteries are used in conjunction with SCs due to the very high cyclability and the significant better temperature domain of the latter, as seen in Tables 1-3. But, in order to provide such hybrid solution means to increase the complexity of the HESS, because the control of the power flows requires appropriate switching of power lines between the different types of HESS components depending on their status. Thus, on one hand, the power electronics should be conceived such as to minimize the commutation loses, and on the other, the thermal management of whole system should be also taken into consideration. In case of transitory functioning regimes the temperature management is of secondary importance, as the sizing of HESS components becomes of primary concern. If, when designing the application, we consider a hybrid solution based on pseudo-supercapacitors, see Table 2, it is important to understand that these devices are not controllable, and this may affect significantly the performance of the system as a whole. Also, it is important to consider the cellularity feature of the storage system that makes it mandatory to preserve the

corresponding balancing of voltage and charge between the energy storage components [16, 17, 18, 19].

When designing a vehicle with HESS, one of the best compromises in overall performance can be found between SCs and batteries, especially in terms of dynamics [9].

III. HESS APPLICATIONS

The hybrid solutions proposed herein are closely correlated with the applications specific. The paper evokes two kinds of applications: i. an application that functions mainly in transitory regime: a heavy shunting diesel hydraulic locomotive and ii. an e-bike that represents a typical application on e-mobility.

A. Starting system of a heavy shunting diesel locomotive with HESS

The main goal of the starting system of the locomotive consists in the injection of a high amount of energy for a very short period of time in order to optimize the starting conditions of the diesel engine. Figure 1 illustrates the simplified energetic circuit of the HESS used for the starting of the heavy shunting locomotive. In order to generate a high angular acceleration at the beginning of the starting process the SC is discharged on the DC series armature motor by using a thyristor electronic switch 1 [19].

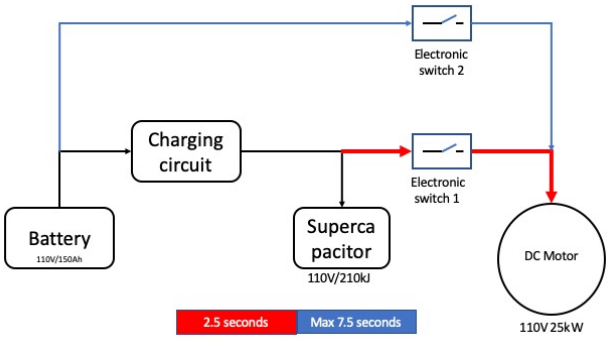

Fig. 1. Simplified energetic circuit of the locomotive HESS.

As Figure 1 illustrates, there are two supply circuits for the starting electrical motor. The first corresponds to the supplying from supercapacitor (switch 1 = ON), after its charging, and the second corresponds to the supply from battery (switch 2 = ON). The strokes produced by the diesel engine when starting are visible as oscillations of the voltage and the current, as will be seen in Figure 6. This feature was used for detecting the revolution speed of the ICE. By implementing switch 1 with a thyristor a secure commutation process is assured. Also, loses and costs of this circuit element are minimized. Switch 2 is implemented with an IGBT. This element applies a reverse voltage on switch 1 switching it off. The control system was significantly simplified due to this solution. Therefore, a very secure and reliable commutation process was obtained.

The rotation speed control for the heavy shunting diesel hydraulic locomotive (LDH1250HP) is assured by a centrifugal inertial regulator. This regulator requires an interval from 2 to 3 seconds in order to reach the steady state regime. The supercapacitor component is sized so as to offer the first power shot necessary only for a certain high acceleration. This favorizes the explosion of the diesel fuel in the ICE cylinders. Afterward, in order to keep the starting electric motor energized, the voltage of the battery, and implicitly the power, is applied in order to reach the ICE steady state regime (minimum stable rotation speed). The simplicity of the control system guarantees a high reliability and reproducibility of the starting conditions for the ICE for a wide temperature domain, from –30°C to more than +50°C. For the simplicity of the system a contribution was brought by the DC mixed series/parallel excitation electrical machine. It was used as a motor in the starting phase of locomotive diesel engine, and afterward it was used as an electric generator for the train services. This combination allows a very high pulse current in the initial phase followed by a relatively reduced value of the current until the diesel engine reaches the stable rotation speed regime.

This implementation uses stacked aqueous electrolyte (KOH) supercapacitors (3x12F/110V) with a total energy capacity of 217.800 kJ. The supercapacitor technology used is an older one, but the mechanical dynamics features of the SC are exceptional. It supports more than 10g shocks and more than ±5g sinus vibrations for 1,000 hours. The functioning temperature domain is between -40°C and more than +60°C, which complies with the rolling rail standards. In comparison with the initial storage system (based only on battery), our implementation uses less than half of the battery capacitance (360Ah vs 150Ah) and the functioning voltage is significantly better: 90V, which is less than the nominal voltage of the locomotive (96V is the nominal voltage and 110V is the maximum voltage). Multiple tests were performed in extreme conditions including completely depleted batteries, even with some of the cells damaged, starting from a voltage of 86÷90V on the batteries. In all of these tests the locomotive was securely started. The tests demonstrated an exceptional availability and reliability of the designed locomotive starting system [16, 17, 18, 19].

The equation of the series armature motor [20, 21, 22] is given by:

$$V_a = k \cdot \Phi_m \cdot \Omega_a + R_a \cdot I_a + R_u \cdot I_a \quad (1)$$

$$T_a = k \cdot \Phi_m \cdot I_a \quad (2)$$

In equation (1) k is a DC machine constant. Φ_m is the magnetic field inside the electrical machine. The magnetic circuit of the electrical machine could reach or not the saturation of the magnetic circuit. Ω_a is the rotation speed and R_u is the external electric resistance, which is in our case:

$$R_u = R_{SC\text{-}ESR} + R_{on\text{-}SCR} + R_w \quad (3)$$

In equation (3) $R_{SC\text{-}ESR}$ is the supercapacitor equivalent series resistance, $R_{on\text{-}SCR}$ is the SCR in conduction resistance and R_w represents the connection wires resistance. Without saturation the magnetic flux is linear with the current:

$$k \cdot \Phi_m \cdot I_a = k' \cdot I_a \quad (4)$$

Respectively it is linear with I_a. By replacing in equation (1), it results that:

$$I_a = V_a / (R_a + R_u + k' \cdot \Phi_m) \text{ and } T_a = k' \cdot I_a^2 \quad (5)$$

By replacing I_a with T_a in equation (5), the torque produced by machine is given by:

$$T_a = k' \cdot V_a / (R_a + R_u + k' \cdot \Phi_m)^2 \quad (6)$$

The movement equation of the starting system is given by:

$$J_{red} \cdot (d\omega / dt) + k_v \cdot \omega = T_a + T_{ICE} \quad (7)$$

In equation (7) J_{red} is the reduced inertia momentum at the electrical machine's shaft, ω is the is the revolution speed, k_v is the viscous friction, T_a represents the electrical machine torque and T_{ICE} represents the torque produced by ICE. During the starting process, the strokes produced by fuel that ignite periodically will reverse the value of T_{ICE} as a result of the strokes produced by fuel ignition and burning inside the locomotive cylinders. Thus, the role of the electrical machine will alternate from motor to generator and vice versa during the starting of the locomotive's ICE. As a consequence, the electrical machine equation will alternate periodically between the form in equation 1 and the form that is given by:

$$V_a = k \cdot \Phi_m \cdot \Omega_a - R_a \cdot I_a + R_u \cdot I_a \quad (8)$$

From the mechanical and thermo-dynamical point of view the locomotive diesel engine has the following constructive data: - it assures a maximum revolution speed of 750 r/min; - it has 6 cylinders "in line" with 133 liters capacity, a mean compression ratio value of 11.25, a piston range' displacement of 360 mm, a cylinder diameter of 280 mm, a mean linear speed of the piston 9 m/s, an ignition revolution speed of 170-180 r/min, and a minimum revolution speed of 325 r/min regulated by a centrifugal speed regulator. The necessary torque at start is around 7.6 kNm. The successive ignition of the cylinder is: 1-5-3-6-2-4. The pressure varies from 57 daN/mm^2 (at 750 r/min) to 29.4 daN/mm^2 (at 325 r/min). At the ignition moment the resistant torque is around 2.2 kNm.

The crank mechanism illustrated in Figure 2. The pressure inside the engine cylinder is illustrated in Figure 3.

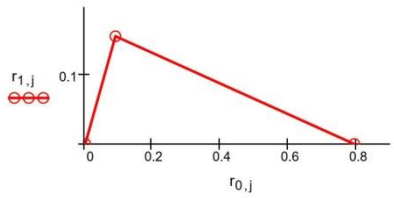

Fig. 2. Crank mechanism illustrating the transformation or rotation of arm $r_{1,j}$ in linear displacement $r_{0,j}$ (coordinates are relative)

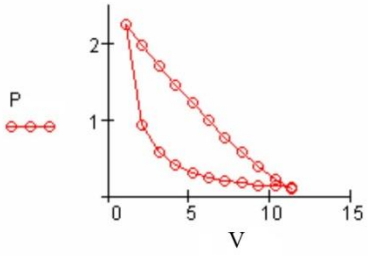

Fig. 3. PV (pressure-volume) diagram of fuel inside engine cylinder at compression (coordinates are relative)

As a consequence of the fuel ignition inside cylinders, the torque variation for this particular engine is shown in Figure 4.

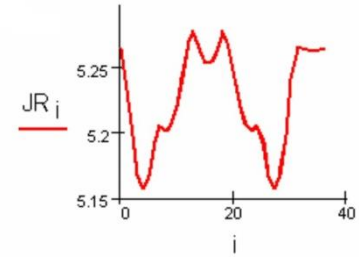

Fig. 4. Reduced momentum JR (in kgm^2) at engine shaft during the first 40 calculation steps (10 degrees per step)

B. Proof of concept e-bike with HESS

Among small and medium personal EVs, e-bikes have a battery disposal impact that is two to three times higher than that of big and medium e-scooters [9]. In order to reduce this battery dependency and avoid battery losses, e-bikes with HESS could be seen as a real alternative, especially by adding storage elements such as SC. The e-bike's life span is quite similar to the normal bike's life span.

Two different solutions for HESS were tested. The first introduces only a boost-buck DC/DC converter in order to control the power flow transfer between SC and the common power bus (V_{rail}) that supplies the motor inverter. The control is implemented using a microcontroller-based system. The block diagram is illustrated in Figure 5.

The bidirectional DC-DC power converter control is inserted between the supercapacitor, which is a part of the HESS, and the power rail of the e-bike directly connected to the battery. Its role is to assure the adequate power flow control of the e-bike motor and to extract from the supercapacitor the stored energy during the acceleration period.

By inserting in the batteries circuit a diode in series at its output, as seen in Figure 5, the overvoltage settled on the output of the bidirectional converter is $V_{GM} = V_{Bat} + \Delta V_{DC\text{-}DC}$, where $\Delta V_{DC\text{-}DC} > 0$ and this voltage is bigger than the batteries' output voltage. It is provided by the supercapacitor via DC-DC converter. The current consumed by the Golden Motor PIE5 system will be given by the power supplied to the e-bike, and the current consumed is given by:

$$I_{GM} = P_{GM} / V_{rail} \quad (9)$$

where: $V_{rail} = V_{Bat} + \Delta V_{DC\text{-}DC} = V_{GM}$ (10)

This current will be converted from SC by the DC-DC converter and will generate the discharge of the supercapacitor. Normally, the control system will discharge until half of the initial voltage the SC, which is 16V.

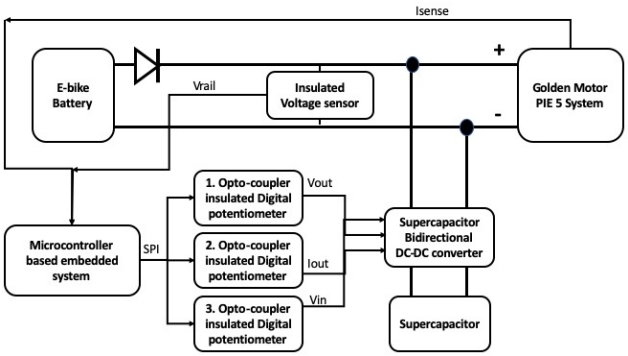

Fig. 5. Block diagram of HESS control system for e-bike prototype

The overall efficiency of the DC-DC converter is provided by:

$$\varepsilon = P_{GM} / P_{SC} \quad (11)$$

In equation (11) P_{SC} is the power transferred from SC, and P_{GM} is the power consumed by the Golden Motor system. The current provided by SC during the starting period will be given by:

$$i_{SC}(t) = V_{SC}(t_0) / (R \cdot e^{-t/RC}) \quad (12)$$

$$\text{and } v_{SC}(t) = V_{SC}(t_0)\,(1 - R \cdot e^{-t/RC}) \quad (13)$$

By replacing $v_{SC}(t)$ with $0.5 \cdot V_{SC}(t_0)$ results that the discharging time is:

$$0.5 = e^{-t/RC} \text{ or } ln(0.5) \cdot R \cdot C = -t \quad (14)$$

In equation (14) $t = 0.693 \cdot R \cdot C$. By replacing C with 29F, and by supposing that R is equal with 0.5Ω, it results that the acceleration period supported from supercapacitor will be 10.048 seconds. The microcontroller based on sampled current I_{sense} and voltage V_{rail} will generate the control signals for the voltage overdriving of the Golden Motor PIE 5 system based on a fuzzy algorithm. In this sense, a standard boost-buck converter with presets for input voltage V_{in}, output current limitation I_{out} and output voltage V_{out} was used in order to control the power flow from/to supercapacitor during e-bike' acceleration and deceleration periods. The microcontroller acquires the breaking signal from the e-bike's throttle, the I_{sense} signal from Golden Motor PIE 5 system, and also monitors the voltage rail V_{rail} connected directly to the battery. Using the running program on microcontroller, which depends on biker control and acquired signals (V_{rail}, I_{sense}), the three control signals (V_{in}, V_{out} and I_{out}) applied on the bidirectional DC-DC converter will consequently change the power flow from/to SC unit (29F/32V organic electrolyte).

In order to improve the energy efficiency, the second variant for power flow control is depicted in Figure 6.

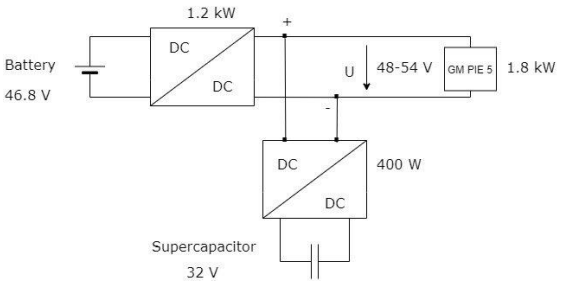

Fig. 6. Block diagram of the double DC-DC converter solution for e-bike with HESS.

The two bidirectional DC/DC converters in Figure 6 offer a closer control of the power flows from both sides. For optimal design, the ratio between battery and SC capacitances was set in order to compensate for the e-bike's maximum kinetic energy by functional SC capacitance. This was obtained also as a result of several measures taken during the design of the system, consisting in replacement of batteries with a hybrid storage solution, adequate sizing of the fast release storage component (SC capacitance) that fully covers the dynamic kinetic energy variation during the e-bike's operation and by appropriate design of the power electronics functions that ensure that the maximum limits are respected by the hybrid storage system.

The sizing process, as shown in the preliminary results obtained for our e-bike, satisfies the reliability and life span requirements foreseen initially. The e-bike's life span depends on exploitation conditions, such as biker's speed profile, daily traveled distance, and thermal behavior of the e-bike's storage system. These interdependences have a major influence on product life cycle (LPC or LLC), reflected by LCA and the performance analyses.

The control of power flows is essential for ensuring the system's energy efficiency, by means of power electronics. The majority of applications, such as e-bike with HESS (or hybrid e-bike), are related to electric mobility. The performance and economic impacts of this implementation were compared to other small and medium EVs, and significant improvements were obtained, as it will be detailed in the next chapter.

IV. Results

Figures 7 and 8 illustrate the variation of voltage and current in two cases: shunting locomotive energized only from batteries (360Ah/96V), and respectively from the hybrid storage system (a combination of the 150Ah/96V battery with the 36F/110V supercapacitor). The blue lines represent the initial case, while the red lines represent the prototype. As an important remark, the commutation from the SC to the battery is produced at 2÷2.5 seconds after the starting moment. Figure 9 shows that the starting moment occurs after 1÷1.5 seconds, and the commutation from SC to battery happens after 4÷5 seconds.

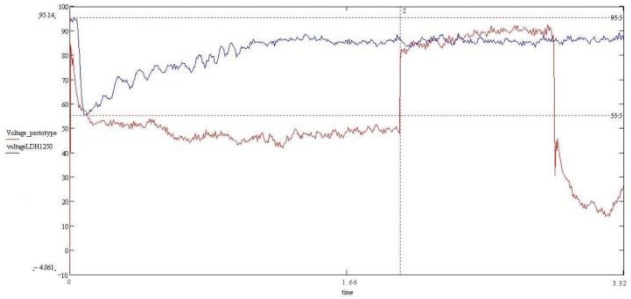

Fig. 7. Voltage variation during the starting process (Y axis: normalized voltage -max. value 95.14 V, X axis: time in seconds); blue initial system, red-prototype endowed with HESS.

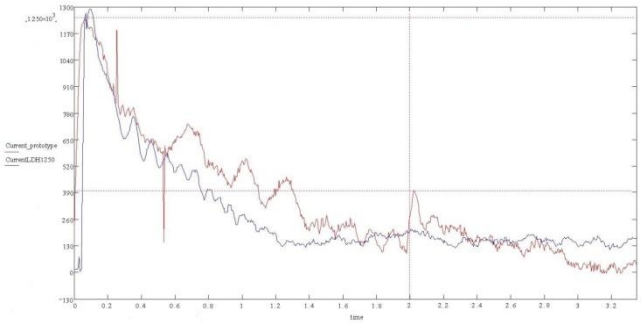

Fig. 8. Current variation during the starting process (Y axis: normalized current -max. value 1250 A, X axis: time in seconds) blue initial system, red-prototype endowed with HESS.

A number of more than 1300 tests were performed on the new starting system endowed with HESS. The tests prove the reliability and availability of the solution. All starting processes of the locomotive were successful even when the battery voltage was very low (around 86÷88V) as illustrated by that several cells that were damaged. The variation of current for the prototype is significantly bigger because of its series equivalent resistance. The bigger current variation illustrates the successive conversions of the electrical starting machine from the motor to the generator regime and vice versa. The series of experimental results also reveal that the temperature of the environment has no significant impact for the prototype (the variation was between -20ºC and +40 ºC).

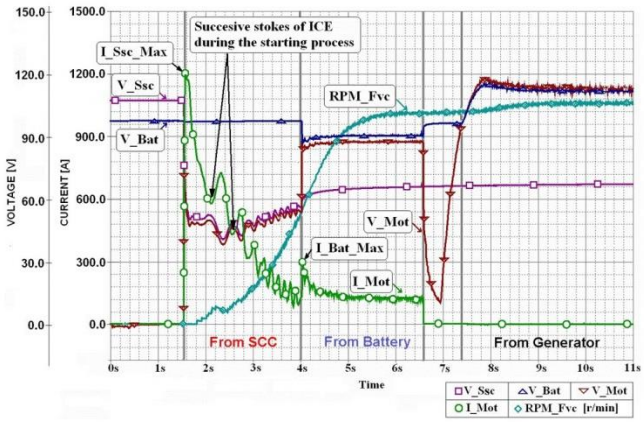

Fig. 9. Main parameters variation during the starting process of the LDH diesel locomotive.

For the e-bike, a compromise was obtained by modifying the ratio between the two storage system component capacitances (battery and SC) [23, 24]. This can represent an optimization method for reaching an overall performance of EVs, and implicitly sustainability goals. We have put in practice this method by developing an e-bike with HESS that is similar in weight (27 kg) to a normal e-bike (20-30kg). It stores more energy than 600 Wh and is able to deliver more power (up to 1800 W, instead of 250–750 W of a normal e-bike), which is at the same level with a big e-bike that weighs around 60–100 kg [9].

V. Discussion and Conclusions

The designed and implemented starting system for the diesel hydraulic prototype endowed with the hybrid storage is illustrated in Figure 10.

Fig. 10. The diesel locomotive LDH1250CP with hybrid storage starting system (based on the SC pack that include Lead-acid batteries)

The prototype was tested for several years providing available and reliable starting processes on the LHD1250HP locomotive. The mean daily fuel savings were more than 25l per 24 hours. Considering the refit costs, the solutions prove a return of investment that was achieved in less than 6 months. Meanwhile, the authors developed an improved solution that senses the fuel ignition inside the cylinders and counts the strokes produced during the starting process. This solution has eliminated the necessity to control the time for the switching moment of the power supply from SC to batteries. Also, by taking into account that the same electrical machine was used for energizing the train, we used the supercapacitors to improve the dynamic behavior of the voltage regulator. We propose that the ratio between the maximum current at initiation of the starting process and the moment when the supply is shifted from SC to battery should be used for illustrating the quality of the starting process. In case of our prototype this ratio was more than 5.8.

Fig. 11. Proof of concept e-bike with HESS.

For the e-bike, we have analyzed our solution in terms of sustainability, mainly energy consumption, autonomy, costs, and battery disposal. Improvements were observed in all of these categories, plus the life span of such a small EV is much better than that of a conventional e-bike: from 1–2 years to 2–4 years, as a result of storage hybridization in conjunction with its appropriate sizing. The authors intend to improve the initial prototype design by developing the dual DC-DC converter solution (see Figure 6) that will allow a better control of the power flow during all dynamic regimes.

ACKNOWLEDGMENT

The authors especially appreciate the discussions and contributions of their colleagues: Pr. Dr. - Eng. Mihai Tofan and Dr. Victor Isaac Herrera. The exchange of experience with them had as a result the improvement of our works. Also, we must acknowledge the Romanian National Research Council that has partially financed our work within the frame program II PNII-018.

REFERENCES

[1] X. Luo, J. Wang, M. Dooner, J. Clarke, "Overview of current development in electrical energy storage technologies and the application potential in power system operation". Appl. Energy, vol. 137, pp. 511–536, 2015.

[2] M. A. Hannan, M. S. H. Lipu, A. Hussain, A. Mohamed, "A review of lithium-ion battery state of charge estimation and management system in electric vehicle applications: Challenges and recommendations". Renew. Sustain. Energy Rev., vol. 78, pp. 834–854, 2017.

[3] J. Libich, J. Máca, J. Vondrák, O. Čech, M. Sedlaříková, "Supercapacitors: Properties and applications". J. Energy Storage, vol. 17, pp. 224–227, 2018.

[4] B. Zakeri, S. Syri, "Electrical energy storage systems: A comparative life cycle cost analysis". Renew. Sustain. Energy Rev., vol. 42, pp. 569–596, 2015.

[5] Y. Li, J. Yang, J. Song, "Electromagnetic effects model and design of energy systems for lithium batteries with gradient structure in sustainable energy electric vehicles". Renew. Sustain. Energy Rev., vol. 52, pp. 842–851, 2015.

[6] Q. Wang, B. Jiang, B. Li, Y. Yan, "A critical review of thermal management models and solutions of lithium-ion batteries for the development of pure electric vehicles". Renew. Sustain. Energy Rev., vol. 64, pp. 106–128, 2016.

[7] A. Muzaffar, M. B. Ahamed, K. Deshmukh, J. Thirumalai, "A review on recent advances in hybrid supercapacitors: Design, fabrication and applications". Renew. Sustain. Energy Rev., vol. 101, pp. 123–145, 2019.

[8] J. M. Baptista, J. S. Sagu, U.W. KG, K. Lobato, "State-of-the-art materials for high power and high energy supercapacitors: Performance metrics and obstacles for the transition from lab to industrial scale—A critical approach". Chem. Eng. J., vol. 374, pp. 1153–1179, 2019.

[9] M. Machedon-Pisu, P. N. Borza, "Are personal electric vehicles sustainable? A hybrid E-bike case study". Sustainability, vol. 12(1). 32, 2020. https://doi.org/10.3390/SU12010032.

[10] F. H. Gandoman, J. Jaguemont, S. Goutam, R. Gopalakrishnan, Y. Firouz, T. Kalogiannis, J. Van Mierlo, "Concept of reliability and safety assessment of lithium-ion batteries in electric vehicles: Basics, progress, and challenges". Appl. Energy, vol. 251, 2019. doi:10.1016/j.apenergy.2019.113343.

[11] J. B. Goodenough, H. D. Abruna, M. V. Buchanan, Basic Research Needs for Electrical Energy Storage. Report of the Basic Energy Sciences Workshop on Electrical Energy Storage. April 2-4, 2007. Office of Basic Energy Sciences Department of Energy. https://doi.org/10.2172/935429

[12] G. Fuchs, B. Lunz, M. Leuthold, D. U. Sauer, Technology Overview on Electricity Storage - Overview on the potential and on the deployment perspectives of electric storage technologies. Institute for Power Electronics and Electrical Drives (ISEA), RWTH Aachen University, 2012. https://doi.org/10.13140/RG.2.1.5191.5925.

[13] H. Chen, T. N. Cong, W. Yang, C. Tan, Y. Li, Y. Ding, Progress in electrical energy storage system: A critical review. Progress in Natural Science, 2009. https://doi.org/10.1016/j.pnsc.2008.07.014.

[14] B. E. Conway, Electrochemical Supercapacitors. Springer, 1999. https://doi.org/10.1007/978-1-4757-3058-6.

[15] F. Beguin, E. Raymundo-Pinero, E. Frackowiak, Carbons for Electrochemical Energy Storage and Conversion Systems. In Advanced Materials and Technologies Series, CRC Press, 2009. https://doi.org/10.1201/9781420055405.

[16] P. Borza, A. M. Puscas, I. Szekely, G. Nicolae, "Energy Management System based on supercapacitors used for starting of internal combustion engines of LDH1250 locomotives and charging their batteries", International Symposium for Design and Technology of Electronic Packages, SIITME, Predeal, Romania, vol. 21, pp. 227-231, 2008.

[17] C. Z. Kertész, P. N. Borza, "Starter aiding system based on supercapacitors for the LDE2100 locomotive". 15th International Symposium for Design and Technology of Electronics Packages (SIITME), 2009. doi: 10.1109/SIITME.2009.5407365.

[18] D. Sojref, P. Borza, "Comparison of high-voltage supercapacitor approaches and case study in diesel locomotive starting system", 3th EESCAP, Rome, 2008.

[19] M. C. Carp, A. M. Puscas, P. N. Borza, "Energy management system and controlling methods for a LDH1250HP diesel locomotive based on supercapacitors". Doctoral Conference on Computing, Electrical and Industrial Systems, Springer, Berlin, Heidelberg, vol. 24, pp. 429-436, 2011.

[20] J. A. Melkebeek, Electrical machines and drives: Fundamentals and advanced modelling. Power Systems (2018th ed.). Springer I. P. AG, 2018. https://doi.org/https://doi.org/10.1007/978-3-319-72730-1.

[21] J. Hindmarsh, A. Renfrew, Electrical machines and drive systems. Newnes Elsevier Science, Linacre House, Jordan Hill, 1996.

[22] T. Wildi, Electrical Machines, Drives, and Power Systems. Fifth Edition (Prentice H). Columbus, Ohio, 2002. https://doi.org/10.1017/CBO9781107415324.004.

[23] D. Shin, Y. Kim, Y. Wang, N. Chang, M. Pedram, "Constant-current regulator-based battery-supercapacitor hybrid architecture for high-rate pulsed load applications". Journal of Power Sources, 2012. https://doi.org/10.1016/j.jpowsour.2011.12.043.

[24] V. I. Herrera, H. Gaztañaga, A. Milo, A. Saez-De-Ibarra, I. Etxeberria-Otadui, T. Nieva, "Optimal Energy Management and Sizing of a Battery-Supercapacitor-Based Light Rail Vehicle with a Multiobjective Approach", IEEE Transactions on Industry Applications, 2016. https://doi.org/10.1109/TIA.2016.2555790.